Ex-vessel neutron dosimetry results in the extended beltline region

Eugene T. Hayes[1,*]

[1]Westinghouse Electric Company LLC, Radiation Engineering & Analysis, 1000 Westinghouse Drive, Cranberry Township, PA 16066, USA

Abstract. Embrittlement of the pressure vessel has been a long-standing concern for pressurized water reactors. Historically, the beltline region of the pressure vessel, or the region of the pressure vessel located opposite the active fuel, has been the primary focus of embrittlement concerns. Embrittlement evaluations typically include a calculation of the neutron flux incident on the pressure vessel, which is in part validated with measurements. In the context of life extension, the beltline region, which is technically defined as the portion of the pressure vessel experiencing fast neutron fluence (E > 1.0 MeV) equal to or greater than 10^{17} n/cm^2, is growing axially. Present fluence calculations for many plants indicate that the beltline region at the end of the 60 years of operation may extend to the bottom of the pressure vessel nozzles. Calculations in the extended beltline are difficult to validate as there are few dosimetry measurements available. At one Westinghouse 4-loop plant, ex-vessel neutron dosimetry sensor sets were irradiated in the extended beltline region. The measurements in the extended beltline region compare well with the discrete ordinates (RAPTOR-M3G) transport calculations and indicate the net uncertainty may be on the order of 30% in the extended beltline region.

1 Introduction

Neutron-induced embrittlement of the reactor pressure vessel has been a long-standing concern for pressurized water reactors. Historically, the beltline region of the pressure vessel, or the region of the pressure vessel located opposite the active fuel, has been the primary focus of evaluations assessing this embrittlement. In the United States, all operating nuclear power plants have a reactor vessel radiation surveillance program based on ASTM E185[1]. In regulator space, neutron-induced embrittlement of the reactor pressure vessel is addressed in Appendix G to 10CFR50 and Appendix H to 10CFR50. Similar requirements exist throughout the world.

The beltline region is defined as the region of the reactor pressure vessel that directly surrounds the effective height of the active core and adjacent regions of the reactor vessel that are predicted to experience sufficient neutron radiation damage to be considered in the selection of the most limiting material regarding radiation damage.

* Corresponding author: hayeset@westinghouse.com

The beltline region is typically defined as the portion of the reactor pressure vessel that will accrue a fast neutron fluence (E > 1.0 MeV) equal to or greater than 10^{17} n/cm^2 at the end of life.

Embrittlement evaluations typically include a calculation of the neutron flux incident on the reactor vessel beltline region, which is in part validated by comparison with dosimetry measurements. Two general types of measurements are commonly used, those being dosimetry sets that are included with the in-vessel surveillance capsules, and at some plants those included in supplemental surveillance programs such as ex-vessel neutron dosimetry.

In the context of life extension, the beltline region is growing axially. Present fluence calculations for many plants indicate that beltline region at the end of the 60 years (or 80 years) of operation may extend to the bottom of the reactor pressure vessel nozzle welds. This extended beltline creates a new problem in terms of validating the neutron fluence calculations in this region well away from the active fuel, in that there are few dosimetry measurements available to confirm calculated results in this new region of interest.

At one Westinghouse 4-loop plant, several ex-vessel neutron dosimetry measurements were made in the extended beltline region. This dosimetry was analysed using three-dimensional discrete ordinates transport theory calculations.

2 Reactor description and transport theory calculations

The neutron transport calculations described in this paper were performed using the RAPTOR-M3G[2] three-dimensional discrete ordinates code and the BUGLE-96 cross section library[3]. RAPTOR-M3G is a Westinghouse developed parallel deterministic radiation transport code that calculates high-resolution neutron flux information. In these calculations, anisotropic scattering was treated with a P_3 Legendre expansion and the angular discretization was modelled with a S_{16} order of angular quadrature.

A section view of the reactor geometry is shown in Figure 1. Also indicated in Figure 1 are the axial locations where ex-vessel neutron dosimetry capsules were located including three locations in the traditional beltline region: the top of the core, the core midplane, and the bottom of the core; and two locations in the extended beltline region: in the vicinity of the reactor vessel supports, and at the elevation of the pressure vessel lower shell to bottom head circumferential weld.

In addition to the core, reactor vessel internals, pressure vessel and biological shield the model included explicit representations of the pressure vessel cladding, pressure vessel reflective insulation, the reactor cavity liner plate, as well as the reactor vessel supports.

In developing the model shown in Figure 1, nominal design dimensions were employed for the various structural components. Water temperatures and hence coolant densities in the reactor core and downcomer region of the reactor were taken to be representative of full-power operating conditions. The reactor core itself was treated as a homogeneous mixture of fuel, cladding, water, and miscellaneous structures such as fuel assembly grids, guide tubes, etc. The r,Θ,z model consisted of 233 radial by 185 azimuthal by 469 axial mesh (~20.2 million mesh). Mesh sizes were chosen to assure that proper convergence of the inner iterations was achieved on a pointwise basis. The pointwise inner iteration flux convergence criterion used in the r,Θ,z calculations was 0.001.

The core power distributions used in the plant-specific transport analysis were taken from appropriate design documentation. The data extracted included fuel assembly specific initial enrichments, beginning of cycle burnups and end of cycle burnups. Appropriate axial distributions were also obtained.

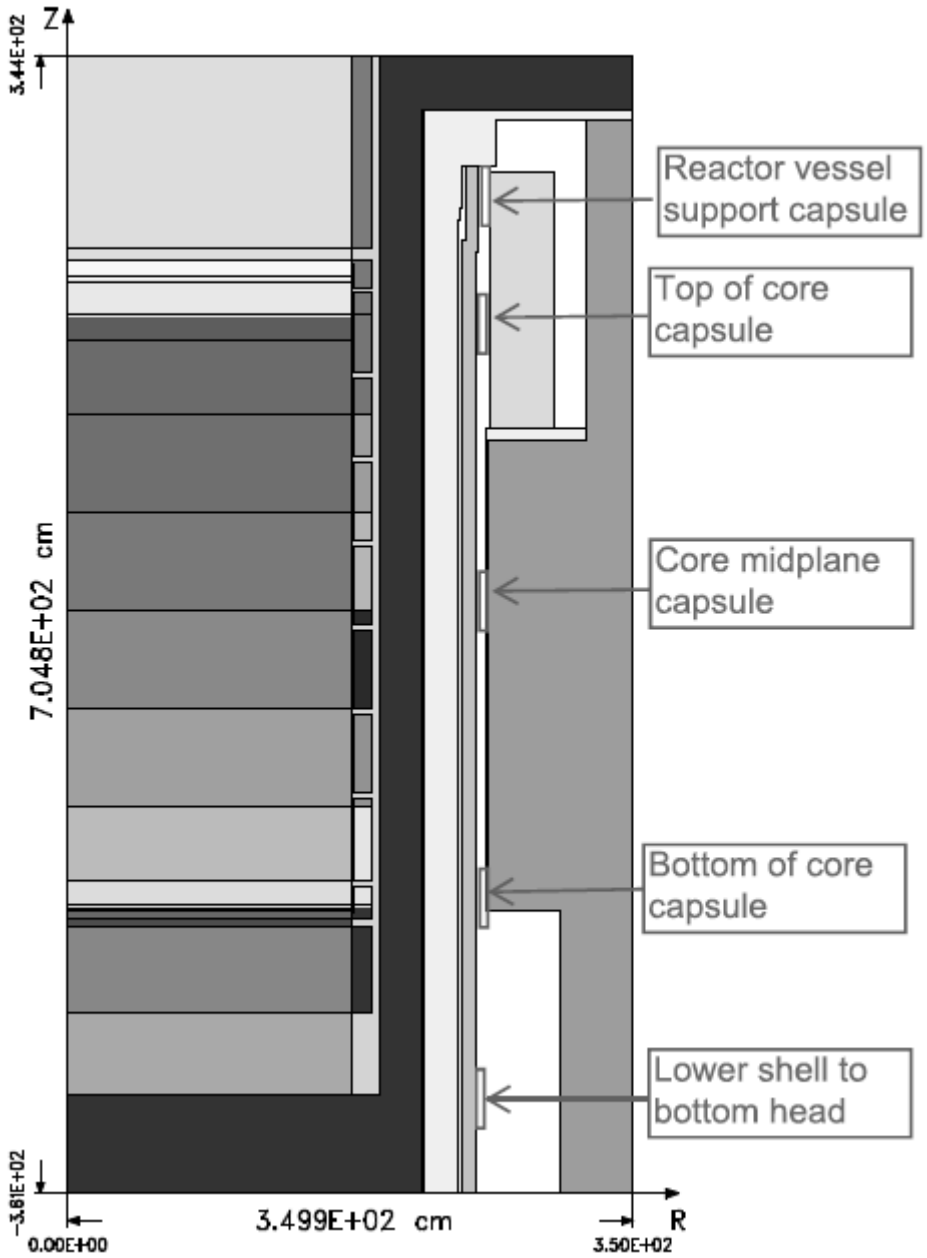

Fig. 1. Reactor geometry and ex-vessel neutron dosimetry locations.

The fuel assembly enrichment and burnup data were used to generate the spatially dependent neutron source throughout the reactor core. This source description included the spatial variation of isotope dependent (U-235, U-238, Pu-239, Pu-240, Pu-241, and Pu-242) fission spectra, neutron emission rate per fission, and energy release per fission based on the burnup history of individual fuel assemblies. These fuel assembly specific neutron source strengths derived from the detailed isotopics were then converted from fuel pin

cartesian coordinates to the r,Θ ,z spatial mesh arrays used in the RAPTOR-M3G discrete ordinates calculations

3 Results of transport calculations

During several cycles of reactor operation, a total of seventeen dosimetry capsules were irradiated in the reactor cavity at two different azimuthal angles and a total of five axial elevations as shown in Figure 1; three locations in the traditional beltline region: the top of the core, the core midplane, the bottom of the core; and two locations in the extended beltline region: in the vicinity of the reactor vessel supports, and at the elevation of the pressure vessel lower shell to bottom head circumferential weld. In addition to the dosimetry capsules, the stainless steel chain connecting them was segmented at one foot (30.48 cm) intervals and counted for additional information regarding the axial gradient.

Table 1 provides a summary of the measurement-to-calculation (M/C) ratios for the five ex-vessel neutron dosimetry capsules located at the core midplane. For the individual threshold foils, the average measurement-to-calculation ratio ranges from 0.91 to 1.08 with an overall average of 0.96 with an associated standard deviation of 9.8%.

In Table 2, similar comparisons are provided for the six sensor sets withdrawn from locations opposite the top and bottom of the active fuel stack. For the individual threshold foils, the average measurement-to-calculation ranges from 0.87 to 1.01 with an overall average of 0.95 and a standard deviation of 12%.

Table 1. Measurement-to-calculation reaction rates for midplane capsules.

Reaction	Dosimetry Capsule ID					Average	% Std. Dev.
	1	2	3	4	5		
^{63}Cu (n,α) ^{60}Co	1.02	0.96	0.87	0.86	0.93	0.93	7.1
^{46}Ti (n,p) ^{46}Sc	1.01	0.96	0.88	0.89	0.91	0.93	5.8
^{54}Fe (n,p) ^{54}Mn	1.04	0.99	0.89	0.89	0.88	0.94	7.7
^{58}Ni (n,p) ^{58}Co	0.99	0.92	0.87	0.87	0.89	0.91	5.5
^{238}U (n,f) ^{137}Cs	1.07	1.07	--	--	--	1.07	0.0
^{93}Nb (n,n') ^{93m}Nb	--	--	1.25	0.93	1.04	1.07	15
^{237}Np (n,f) ^{137}Cs	1.10	1.06	--	--	--	1.08	2.6
Average of M/C Results						**0.96**	**9.8**

Table 2. M/C reaction rates for capsules located at the top and bottom of the fuel stack.

Reaction	Dosimetry Capsule ID						Average	% Std. Dev.
	6	7	8	9	10	11		
^{63}Cu (n,α) ^{60}Co	0.86	1.01	0.79	0.90	0.77	0.86	0.87	9.9
^{46}Ti (n,p) ^{46}Sc	0.94	1.10	0.91	1.09	0.97	1.04	1.01	7.9
^{54}Fe (n,p) ^{54}Mn	0.83	1.06	0.80	0.99	0.79	0.95	0.90	12
^{58}Ni (n,p) ^{58}Co	0.90	1.11	0.91	1.06	0.92	1.04	0.99	9.2
^{238}U (n,f) ^{137}Cs	0.85	1.14	--	--	--	--	1.00	21
^{93}Nb (n,n') ^{93m}Nb	--	--	0.83	1.03	0.87	1.09	0.96	13
^{237}Np (n,f) ^{137}Cs	0.89	1.11	--	--	--	--	1.00	16
Average of M/C Results							**0.95**	**12**

For the extended beltline region, Table 3 provides the comparisons of the measurement-to-calculation ratios for the five sensor sets withdrawn from the vicinity of the reactor vessel supports, while the results for the two capsules withdrawn from measurement locations opposite the pressure vessel lower shell to bottom head circumferential weld are provided in Table 4.

Table 3. M/C reaction rates for capsules near the reactor vessel supports.

Reaction	Dosimetry Capsule ID					Average	% Std. Dev.
	12	13	14	15	16		
^{63}Cu (n,α) ^{60}Co	0.68	--	0.60	0.60	0.53	0.60	10
^{46}Ti (n,p) ^{46}Sc	0.76	0.65	0.69	0.73	0.59	0.68	9.8
^{54}Fe (n,p) ^{54}Mn	0.76	0.67	0.66	0.63	0.49	0.64	15
^{58}Ni (n,p) ^{58}Co	0.78	0.68	0.68	0.74	0.54	0.68	13
^{238}U (n,f) ^{137}Cs	1.09	0.92	--	--	--	1.01	12
^{93}Nb (n,n') ^{93m}Nb	--	--	1.33	1.02	0.58	0.98	39
^{237}Np (n,f) ^{137}Cs	1.18	0.82	--	--	--	1.00	26
Average of M/C Results						**0.75**	**28**

Table 4. M/C reaction rates for capsules located opposite the lower shell to bottom head girth weld.

Reaction	Dosimetry Capsule ID		Average	% Std. Dev.
	17	18		
^{63}Cu (n,α) ^{60}Co	1.28	1.03	1.16	15
^{46}Ti (n,p) ^{46}Sc	1.11	0.94	1.03	12
^{54}Fe (n,p) ^{54}Mn	1.00	0.87	0.94	9.8
^{58}Ni (n,p) ^{58}Co	1.03	0.90	0.97	9.5
^{93}Nb (n,n') ^{93m}Nb	1.20	0.88	1.04	22
Average of M/C Results			**1.02**	**13**

Corresponding measured and calculated ^{54}Fe (n,p) ^{54}Mn reaction rates are presented in Figure 2 and Figure 3 at two azimuthal locations.

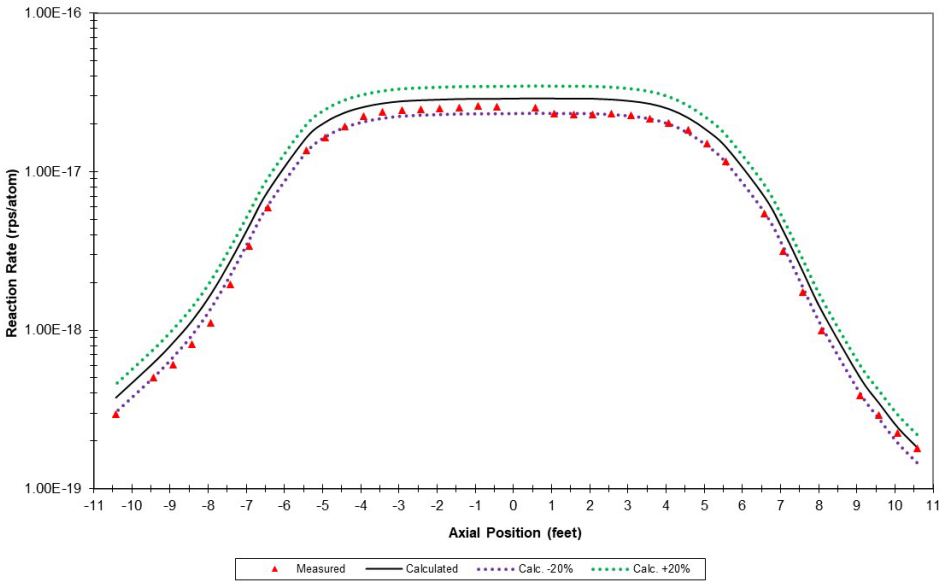

Fig. 2. Measured and calculated iron reaction rate for the stainless steel gradient chain at 0 degrees.

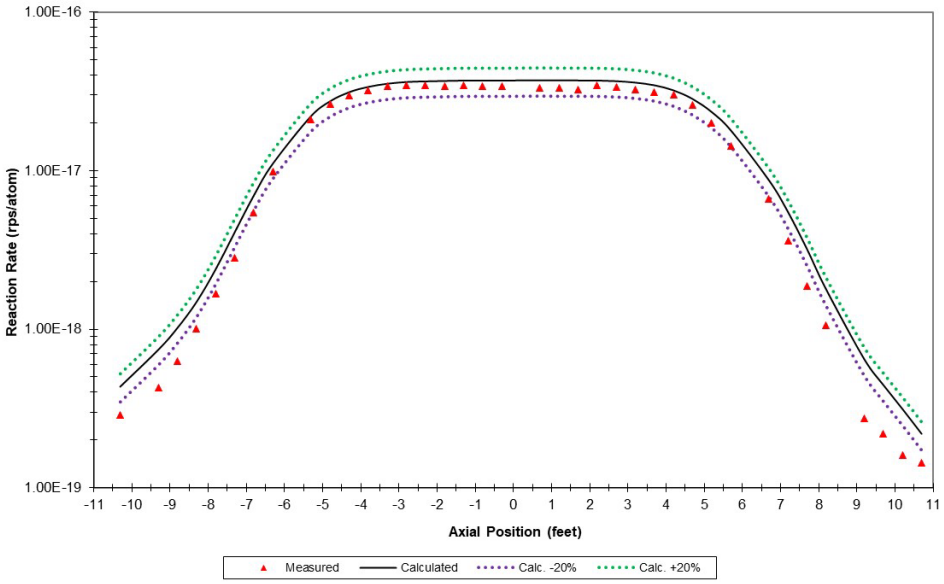

Fig. 3. Measured and calculated iron reaction rate for the stainless steel gradient chain at 45 degrees.

4 Conclusions

In general, the extended beltline measurements compare well with the transport calculations. The benchmarking data set for the extended beltline region evaluated thus far is small; however, it seems that, after combining the results with the expected results of a comprehensive analytic uncertainty assessment, the net methodology uncertainty for the RAPTOR-M3G methodology may be on the order of 30% in the extended beltline region.

One area worth further investigation would be in the vicinity of the reactor vessel supports. As shown in Table 3, the calculations over predict the neutron exposure, especially at the high end of the energy spectrum. The bottom of the 90% neutron response range for the copper, titanium, iron, and nickel dosimeters is 4.53 MeV, 3.70 MeV, 2.27 MeV, and 1.98 MeV, respectively. Neutrons with this much energy constitute a small fraction of the neutron fluence (E > 1.0 MeV) in the extended beltline region.

References

1. ASTM E185-21, “Standard Practice for Design of Surveillance Programs for Light-Water Moderated Nuclear Power Reactor Vessels,” ASTM International, West Conshohocken, PA, 2021, https://doi.org/10.1520/E0185-21
2. G. Longoni and S.L. Anderson, “Reactor Dosimetry Applications Using RAPTOR-M3G: A New Parallel 3-D Radiation Transport Code,” Proceedings of the 13th International Symposium on Reactor Dosimetry, Akersloot, Netherlands, May 25th – May 28th, 2008, pp. 722-732
3. ORNL RSICC Data Library Collection, DLC-185, “BUGLE-96, Coupled 47 Neutron, 20 Gamma-Ray Group Cross Section Library Derived from ENDF/B-VI for LWR Shielding and Pressure Vessel Dosimetry Applications,” March 1996